

Magnetic Flux Tuning of Spin Chirality in Mott Insulators with Ring Exchanges

Yi-Fei Wang¹ and Chang-De Gong^{1,2}

¹Center for Statistical and Theoretical Condensed Matter Physics,
and Department of Physics, Zhejiang Normal University, Jinhua 321004, China

²National Laboratory of Solid State Microstructures and Department of Physics, Nanjing University, Nanjing 210093, China

(Dated: November 3, 2018)

A manifestation of the many-body Aharonov-Bohm effect in the magnetic-flux-tuned Mott insulators with three-spin and four-spin ring exchanges, presents as an effective tool to manipulate the ground-state spin chirality, such as, tune the magnitude continuously, switch an abrupt jump, or even reverse its sign. Such a mechanism is demonstrated explicitly in both quasi-one-dimensional ladders and two-dimensional lattices with triangles as elementary plaquettes.

PACS numbers: 71.10.Hf, 75.10.Jm, 72.80.Sk, 75.50.Ee

Introduction.—Mott insulators (MIs), as the paradigm of strongly correlated materials, have been commonly considered to have only magnetic properties at low energies due to their spin moments. However, it has been demonstrated recently by Bulaevskii *et al.* [1] that, due to a certain form of charge fluctuations, geometrically frustrated MIs may exhibit electric orbital currents accompanying spin textures with chirality. This notion of spin chirality itself has already been an intriguing topic for decades in quantum magnetism, superconductivity and anomalous Hall effect [2]. And the effective spin Hamiltonian of MIs may contain a linear coupling of the spin chirality to an external magnetic field, as proposed by Motrunich [3] when studying the organic compound κ -(ET)₂Cu₂(CN)₃ in which possible spin liquids with spinon Fermi surfaces are of particular interest [4, 5, 6, 7].

At the heart of the theories by Bulaevskii *et al.* and Motrunich [1, 3], it is the three-spin ring exchange (3SRE) in addition to the Heisenberg antiferromagnetic (AFM) two-spin coupling, which is a specific form of charge fluctuations in MIs [8, 9]. This multiple-spin exchange concept, initiated by Thouless [10], now appears as essential in various strongly-correlated systems: bcc solid ³He [11], solid ³He films adsorbed on graphite [12, 13], two-dimensional (2D) electron Wigner crystals [14, 15], and zigzag Wigner crystals in quantum wires [16]. Several experiments have confirmed the presence of four-spin ring exchange (4SRE) in cuprates [17, 18]. And loading cold atoms into optical lattices opens another avenue to design ring exchanges [19].

Despite the above encouraging advances, one still has no quantitative understanding that how can we effectively manipulate the spin chirality in MIs with ring exchanges. It is both of interest and timely to address this problem, and here we conduct such a study of a frustrated spin-1/2 system with 3SRE and 4SRE modulated by a magnetic flux. Employing exact diagonalization (ED) of finite systems, we consider both a (two-leg) triangular ladder and a 2D triangular lattice geometry with periodic boundary conditions (PBCs), which are the simplest systems on which both 3SRE and 4SRE are possible.

Beyond the weak-magnetic-flux regime, we explore the large parameter space systematically, and demonstrate that: at specific combinations of exchange interactions, varying the magnetic flux strength enable us to tune continuously the magnitude, switch an abrupt jump, or even change the sign, of the ground-state (GS) spin chirality.

Model Hamiltonian.—With the nearest-neighbor (NN) Heisenberg AFM coupling, the 3SRE and 4SRE terms modulated by a uniform magnetic flux, the spin-1/2 model Hamiltonian in a triangular ladder/lattice reads

$$H = J \sum_{\langle ij \rangle} \mathbf{S}_i \cdot \mathbf{S}_j - K_3 \sum_{ijk \in \triangle} \left[e^{i\phi} P_{ijk} + e^{-i\phi} P_{ijk}^{-1} \right] + K_4 \sum_{ijkl \in \diamond} \left[e^{i2\phi} P_{ijkl} + e^{-i2\phi} P_{ijkl}^{-1} \right] \quad (1)$$

where \mathbf{S}_i is the spin operator on site i . P_{ijk} which defined as $P_{123} : |\sigma_1, \sigma_2, \sigma_3\rangle \rightarrow |\sigma_3, \sigma_1, \sigma_2\rangle$, is the cyclic permutation of the three spins sitting on a triangular plaquette, and satisfies $P_{123}^{-1} = P_{123}^\dagger = P_{321}$. And similarly $P_{1234} : |\sigma_1, \sigma_2, \sigma_3, \sigma_4\rangle \rightarrow |\sigma_4, \sigma_1, \sigma_2, \sigma_3\rangle$ is the cyclic permutation of the four spins sitting on a rhombus consisting of two elementary triangles. The three sums in Eq. (1) run, respectively, over all NN bonds, elementary triangles and rhombi. Contrary to ³He systems in which the ³He atoms are neutral, and similar to electron Wigner crystals [20], a magnetic flux through the exchange path can change the nature of the ring exchanges in MIs, owing to the Aharonov-Bohm (AB) effect. ϕ is the magnetic flux treading a triangular plaquette, in units of $\phi_0/2\pi$ ($\phi_0 = hc/e$ is the flux quantum). We focus on the physical parameter space with $J, K_3 > 0$ and $K_4 \geq 0$, and vary the ratio J/K_3 and K_4/K_3 with the setting $K_3 = 1$ (as an energy unit) in the following calculations.

For our spin-1/2 case, P_{ijk} can also be written in terms of electron operators as $P_{123} = (c_{1\alpha}^\dagger c_{1\beta})(c_{2\beta}^\dagger c_{2\gamma})(c_{3\gamma}^\dagger c_{3\alpha})$, and satisfies $i(P_{123} - P_{321}) = -4\mathbf{S}_1 \cdot \mathbf{S}_2 \times \mathbf{S}_3 \equiv -4\chi_{123}$, where χ_{ijk} represents the local spin chirality [2]. In previous studies where a magnetic flux is absent, the 3SRE term itself favors ferromagnetism (FM) and can be taken into account just by modifying J and allowing both $J > 0$

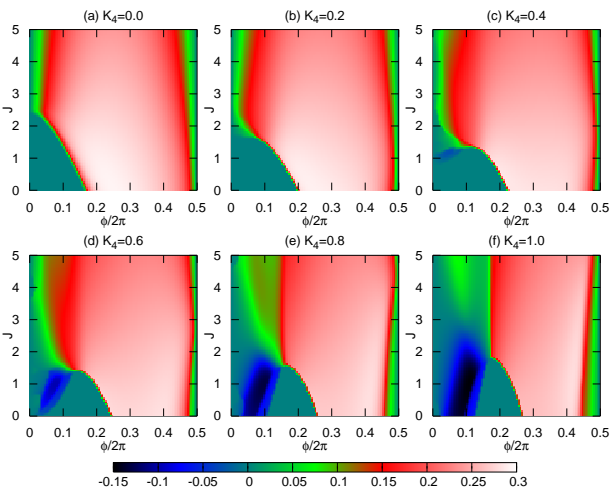


FIG. 1: (color online). Intensity plots of the GS spin chirality χ_0 in the ϕ - J parameter space (setting $K_3 = 1$) of the 8×2 triangular ladder at various fixed 4SRE strengths K_4 's.

and $J \leq 0$ [12, 13]. However even for a small ϕ , since $e^{i\phi}P_{123} + e^{-i\phi}P_{321} = \cos\phi(P_{123} + P_{321}) - 4\sin\phi(\mathbf{S}_1 \cdot \mathbf{S}_2 \times \mathbf{S}_3) \simeq (P_{123} + P_{321}) - 4\phi\chi_{123}$, the magnetic flux couples linearly to the spin chirality in the low- ϕ limit [1, 3, 9], and therefore could probably induce a non-zero chirality density. Here we are concerned with the parameter space of $\phi \in [0, \pi]$, and hence consider the many-body AB effect induced by a strong magnetic flux.

Triangular ladders.—We firstly consider the ladder geometry. We study the GS averaged (local) spin chirality $\chi_0 \equiv -\langle \chi_{ijk} \rangle_0$ (here a negative sign is added for convenience) by varying ϕ , J and K_4 . The typical ED results for a triangular ladder of the size 8×2 are shown in Fig. 1.

In the absence of 4SRE ($K_4 = 0$), χ_0 is non-negative in the parameter region $\phi \in [0, \pi]$, as shown in Fig. 1(a). Note that χ_0 has the symmetry $\chi_0(\phi) = -\chi_0(-\phi) = -\chi_0(2\pi - \phi)$, which has been numerically confirmed. The whole ϕ - J parameter space is roughly separated into two regions: the bottom left corner ($J \lesssim 2.4$, $\phi/2\pi \lesssim 0.17$, and uniformly colored) with $\chi_0 = 0$ and saturated FM ($S_{\text{tot}} = S_{\text{max}}$), and larger region with $\chi_0 > 0$ and spin-singlet GSs ($S_{\text{tot}} = 0$). The quantum critical line between these two regions has also been verified through tracking the non-analyticities in the GS energy function $E_0(\phi, J)$. Later, we will show that the quantum critical line does not depend appreciably on the ladder size.

For the triangular ladders with PBCs, because of the identity $P_{123} + P_{321} = 2\mathbf{S}_1 \cdot \mathbf{S}_2 + 2\mathbf{S}_2 \cdot \mathbf{S}_3 + 2\mathbf{S}_3 \cdot \mathbf{S}_1 + 1/2$, the Hamiltonian with $K_4 = 0$ will reduce to $H = -N \cos\phi + \tilde{J}_1 \sum_{\langle ij \rangle}^{\text{inter}} \mathbf{S}_i \cdot \mathbf{S}_j + \tilde{J}_2 \sum_{\langle ij \rangle}^{\text{intra}} \mathbf{S}_i \cdot \mathbf{S}_j + 4 \sin\phi \sum_{ijk \in \Delta} \mathbf{S}_i \cdot \mathbf{S}_j \times \mathbf{S}_k$ with $\tilde{J}_1 = J - 4 \cos\phi$ and $\tilde{J}_2 = J - 2 \cos\phi$, where the superscript ‘‘inter’’ (‘‘intra’’) corresponds to the effective interchain (intrachain) two-spin coupling \tilde{J}_1 (\tilde{J}_2). At the left boundary line of Fig. 1(a) with $\phi = 0$, there is a

quantum critical point $J \approx 2.4$ corresponding to $\tilde{J}_2/\tilde{J}_1 = -0.25$ which separates the saturated FM phase [21] and the dimer phase [22]. And at the right boundary line of Fig. 1(a) with $\phi = \pi$, the GS is also the dimer phase since $J \geq 0$ and $\phi = \pi$ gives $\tilde{J}_2/\tilde{J}_1 \geq 0.5$ [23]. The features of these states will be displayed and discussed later by various correlation functions.

In the presence of 4SREs, there are even more interesting behaviors of χ_0 , as shown in Figs. 1(b)-(f) with five typical K_4 's respectively. At $K_4 = 0.2$ [Fig. 1(b)], the saturated FM region shrinks in the J direction while expand a little in the ϕ direction. At $K_4 = 0.4$ and $K_4 = 0.6$ [Figs. 1(c) and (d)], at the center of saturated FM region, there appears a negative- χ_0 region in which the GSs are spin singlets ($S_{\text{tot}} = 0$). When K_4 is further increased to 0.8 [Fig. 1(e)] and 1.0 [Fig. 1(f)], the negative- χ_0 region continues to expand and occupies a significant portion in the ϕ - J parameter space.

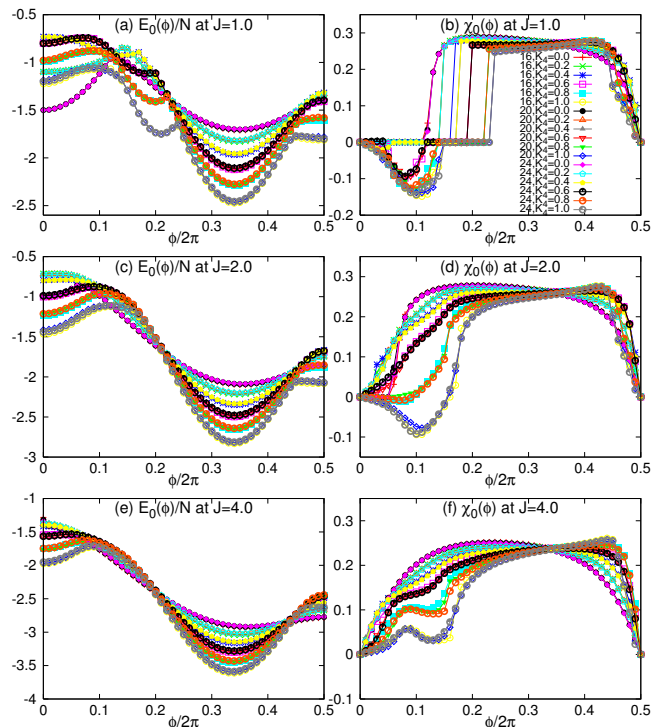


FIG. 2: (color online). Triangular ladders: GS energy per site E_0/N (left) and GS spin chirality χ_0 (right) versus ϕ , for various J 's, K_4 's and ladder sizes N 's.

An intuitive analysis for $K_4 > 0$ is much more difficult, than that in the simpler case of $K_4 = 0$. However, it should be noted that the 4SRE operators satisfy $P_{1234} - P_{4321} = \frac{1}{2}(P_{123} + P_{234} + P_{341} + P_{412} - \text{H.c.}) = 2i(\chi_{123} + \chi_{234} + \chi_{341} + \chi_{412})$. Therefore, $e^{i2\phi}P_{1234} + e^{-i2\phi}P_{4321} = \cos 2\phi(P_{1234} + P_{4321}) - 2 \sin 2\phi(\chi_{123} + \chi_{234} + \chi_{341} + \chi_{412})$. Due to the opposite signs and the different AB periods of 3SRE and 4SRE terms, the low- ϕ -limit coupling coefficient and the portion of negative- χ_0 region depend on the competitions between them.

In order to address the effects of ladder sizes, we compare three sizes of 8×2 , 10×2 and 12×2 . The mainly considered quantities are χ_0 and the GS energy per site E_0/N . From Figs. 2(a),(c),(e), we can see that the $E_0(\phi)/N$ curves coincide well with each other for all three ladder sizes. And the $\chi_0(\phi)$ curves [Figs. 2(b),(d),(f)] also present us rather identical behaviors. All these results indicate that in the thermodynamic limit ($N \rightarrow \infty$), both $E_0(\phi)/N$ and $\chi_0(\phi)$ will not deviate obviously from these finite-size results.

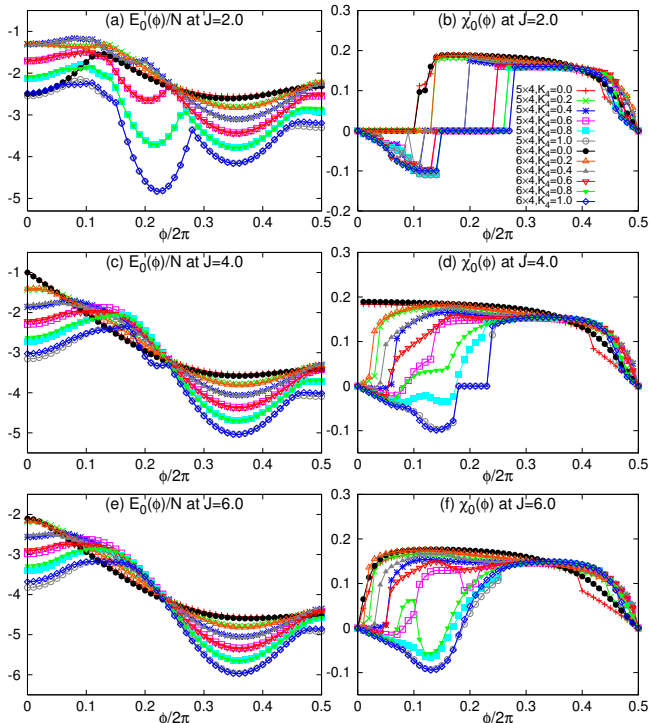


FIG. 3: (color online). Triangular lattices: E_0/N (left) and χ_0 (right) versus ϕ , for various J 's, K_4 's and ladder sizes N 's.

Triangular lattices.—For the 2D triangular lattices, we focus on two cases with the sizes of 5×4 and 6×4 [Fig. 3]. In the absence of 4SRE terms ($K_4 = 0$), similar to the previous case of ladders, the Hamiltonian of a 2D triangular lattice with PBCs will reduce to $H = -N \cos \phi + (J - 4 \cos \phi) \sum_{\langle ij \rangle} \mathbf{S}_i \cdot \mathbf{S}_j + 4 \sin \phi \sum_{ijk \in \Delta} \mathbf{S}_i \cdot \mathbf{S}_j \times \mathbf{S}_k$. From Fig. 3, we can see that $E_0(\phi)/N$ and $\chi_0(\phi)$ display quite similar behaviors resulting from the competitions between 3SRE and 4SRE terms as the ladders, such as the sign changes and abrupt jumps of χ_0 .

Long-range correlations and ordering.—We now turn to three kinds of correlation functions (CFs) in ladders. The first is the spin-spin CF, defined as $C(r) = \langle \mathbf{S}_i \cdot \mathbf{S}_{i+r} \rangle$, where r is the range (in units of the lattice constant) between two sites along the chain direction and takes integer (half-integer) values for intrachain (interchain) spin-spin CF $C_1(r)$ [$C_2(r)$]. The other two CFs are defined as follows [7, 13]. The dimer operator on a bond (i, j) is

defined by $d_{ij} = (1 - P_{ij})/2$ (where P_{ij} exchanges two spins as $P_{12} : |\sigma_1, \sigma_2\rangle \rightarrow |\sigma_2, \sigma_1\rangle$), and this projector gives 1 on a singlet and 0 on a triplet. The dimer-dimer CF between two bonds is $D(r) = \langle d_{ij} d_{kl} \rangle - \langle d_{ij} \rangle \langle d_{kl} \rangle$, and $D_1(r)$ [$D_2(r)$] for two parallel (non-parallel) rung bonds between two chains. The chiral-chiral CF between two triangles is defined as $X(r) = \langle \chi_{ijk} \chi_{lmn} \rangle$, and $X_1(r)$ for two up-triangles (or equivalently two down-triangles), while $X_2(r)$ for an up-triangle and a down-triangle. Note that if the two triangles have some sites in common, $X(r)$ may have a small imaginary part, and only the real part is plotted [13].

At each case when $S_{\text{tot}} = S_{\text{max}} = N/2$, χ_0 always vanishes, and meanwhile $C(r)$ is surely positive and almost a constant at any range r . Now we would take a closer look at the three kinds of CFs of the other cases, and focus on the 12×2 triangular ladder as an example.

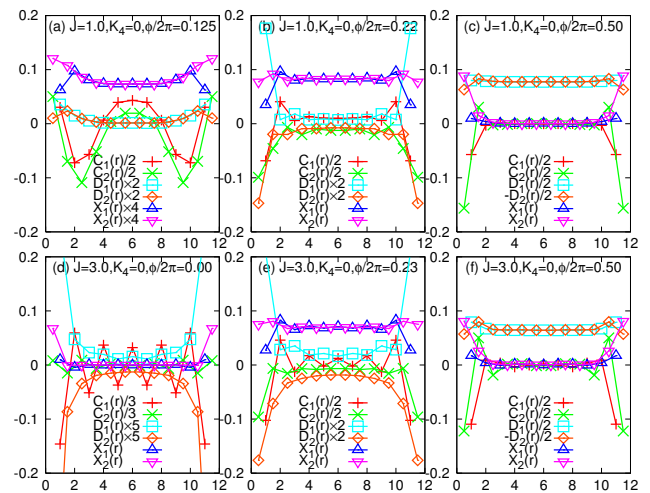


FIG. 4: (color online). Various GS correlation functions (see text) versus the range r of the 12×2 triangular ladders at various J 's, ϕ 's and $K_4 = 0$.

We first consider the simpler cases with only 3SREs (Fig. 4 with $K_4 = 0$). For $J = 1.0$, tuning $\phi/2\pi$ across an FM quantum critical point at 0.125 [Fig. 4(a)], both $C_1(r)$ and $C_2(r)$ exhibit that the GS consists of two-period FM domains with opposite magnetization, which is a remnant signature of long-range FM ordering in the FM region; tuning $\phi/2\pi$ further to 0.22 [Fig. 4(b)] at which $\chi_0(\phi)$ takes a maximum, $C_1(r)$ [$C_2(r)$] shows weak FM (AFM) correlations, and both $X_1(r)$ and $X_2(r)$ reveal nondecaying long-range correlations; when ϕ is increased to π [Fig. 4(c)], $C(r)$'s and $X(r)$'s show fast decaying behaviors, while $D(r)$'s reveal the long-range dimer ordering. For $J = 3.0$, $\phi = 0$ [Fig. 4(d)], $C_1(r)$ [$C_2(r)$] shows strong (weak) AFM correlations because of $\tilde{J}_2 > \tilde{J}_1$, and $D(r)$'s also show slowly decaying correlations; tuning $\phi/2\pi$ to make $\chi_0(\phi)$ take a maximum [Fig. 4(e)] and then to 0.5 [Fig. 4(f)], there kinds of CFs resemble the $J = 1.0$ cases.

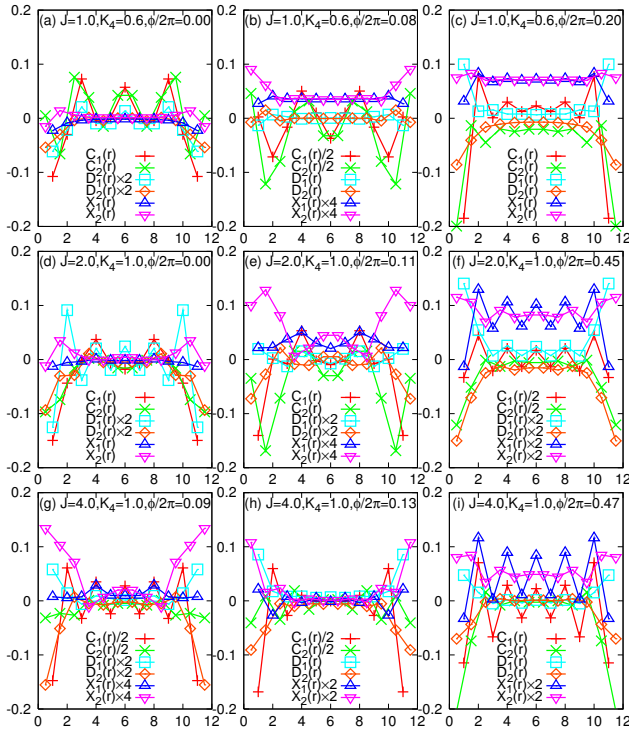


FIG. 5: (color online). The same as Fig. 4, but with nonzero 4SREs ($K_4 > 0$).

Next, we progress to much more complicated and interesting cases with 4SREs (Fig. 5). For $(J, K_4) = (1.0, 0.6)$, at $\phi = 0$ [Fig. 5(a)], the nonzero K_4 makes the long-range FM correlations destroyed, $C(r)$'s and $D(r)$'s exhibit nondecaying fluctuations although $X(r)$'s show fast decaying behaviors; tuning $\phi/2\pi$ to 0.08 [Fig. 5(b)], at which $\chi_0(\phi)$ takes a negative minimum, the $C(r)$'s exhibit FM domains and $X(r)$'s reveal long-range correlations; then tuning $\phi/2\pi$ to 0.20 [Fig. 5(c)], at which $\chi_0(\phi)$ jumps to a large positive value, $X(r)$'s show long-range correlations. For $(J, K_4) = (2.0, 1.0)$, tuning $\phi/2\pi$ to 0.11 [Fig. 5(e)] at which $\chi_0(\phi)$ takes a minimum, the $X(r)$'s show strong two-period fluctuations; tuning $\phi/2\pi$ further to 0.45 [Fig. 5(f)] at which $\chi_0(\phi)$ drops steeply, $X_1(r)$ displays strongly fluctuating correlations, and $C_1(r)$ also shows strong intrachain AFM correlations. For $(J, K_4) = (4.0, 1.0)$, tuning ϕ to 0.09 [Fig. 5(g)] at which $\chi_0(\phi)$ takes a local maximum, the $X(r)$'s show strong two-period fluctuations; when tuning $\phi/2\pi$ to 0.47 [Fig. 5(i)], we can see some behaviors resembling the previous case in Fig. 5(f).

Summary and discussion.—For a spin-1/2 system in a triangular ladder/lattice with NN AFM coupling, 3SRE and 4SRE, and a uniform magnetic flux ϕ , we can effectively manipulate the GS spin chirality χ_0 , such as tune continuously the magnitude of χ_0 by varying ϕ , switch an abrupt jump near an FM phase boundary, or even reverse the sign of χ_0 , and change the low- ϕ -limit cou-

pling coefficient. Various CFs discover the characteristic long-range correlations accompanying the tuned spin chiralities. Such a mechanism presents a peculiar manifestation of the many-body AB effect on quasi-localized spins in MIs. This magnetic flux tuning of spin chirality is expected to be observed in 2D organic compound κ -(ET) $_2$ Cu $_2$ (CN) $_3$, quasi-1D and 2D Wigner crystals, and cold atoms in optical lattices with ring exchanges.

This work was supported by NSFC of China (No. 10904130) and State Key Program for Basic Researches of China (No. 2006CB921802). ED calculations were based on TITPACK Ver. 2 package by H. Nishimori.

-
- [1] L. N. Bulaevskii, C. D. Batista, M. V. Mostovoy, and D. I. Khomskii Phys. Rev. B **78**, 024402 (2008).
 - [2] X. G. Wen, F. Wilczek, and A. Zee, Phys. Rev. B **39**, 11413 (1989); Y. Taguchi *et al.*, Science **291**, 2573 (2001); D. Grohol *et al.*, Nat. Mater. **4**, 323 (2005).
 - [3] O. I. Motrunich, Phys. Rev. B **73**, 155115 (2006).
 - [4] O. I. Motrunich, Phys. Rev. B **72**, 045105 (2005).
 - [5] S.-S. Lee and P.A. Lee, Phys. Rev. Lett. **95**, 036403 (2005).
 - [6] O. I. Motrunich and M. P. A. Fisher, Phys. Rev. B **75**, 235116 (2007).
 - [7] D. N. Sheng, O. I. Motrunich, S. Trebst, E. Gull, and M. P. A. Fisher, Phys. Rev. B **78**, 054520 (2008); D. N. Sheng, O. I. Motrunich, and M. P. A. Fisher, *ibid.* **79**, 205112 (2009).
 - [8] M. Takahashi, J. Phys. C **10**, 1289 (1977); A. H. MacDonald, S. M. Girvin, and D. Yoshioka, Phys. Rev. B **37**, 9753 (1988).
 - [9] D. S. Rokhsar, Phys. Rev. Lett. **65** 1506 (1990); D. Sen and R. Chitra, Phys. Rev. B **51**, 1922 (1995).
 - [10] D.J. Thouless, Proc. Phys. Soc. Lond. **86**, 893 (1965).
 - [11] M. Roger, J.M. Delrieu, J.H. Hetherington, Rev. Mod. Phys. **55**, 1 (1983).
 - [12] T. Momoi, K. Kubo, and K. Niki, Phys. Rev. Lett. **79**, 2081 (1997); K. Kubo and T. Momoi, Z. Phys. B **103**, 485 (1997).
 - [13] G. Misguich, B. Bernu, C. Lhuillier, and C. Waldtmann, Phys. Rev. Lett. **81**, 1098 (1998); G. Misguich, C. Lhuillier, B. Bernu, and C. Waldtmann, Phys. Rev. B **60**, 1064 (1999).
 - [14] M. Roger, Phys. Rev. B **30**, 6432 (1984).
 - [15] B. Bernu, L. Candido, D.M. Ceperley, Phys. Rev. Lett. **86**, 870 (2001).
 - [16] A. D. Kironomos, J. S. Meyer, T. Hikihara, and K. A. Matveev, Phys. Rev. B **76**, 075302 (2007).
 - [17] R. Coldea *et al.*, Phys. Rev. Lett. **86**, 5377 (2001).
 - [18] A. M. Toader *et al.*, Phys. Rev. Lett. **94**, 197202 (2005).
 - [19] H. P. Büchler, M. Hermele, S. D. Huber, M.P.A. Fisher, and P. Zoller, Phys. Rev. Lett. **95**, 040402 (2005).
 - [20] T. Okamoto and S. Kawaji, Phys. Rev. B **57**, 9097 (1998); T. Okamoto, K. Hosoya, S. Kawaji, and A. Yagi, Phys. Rev. Lett. **82**, 3875 (1999).
 - [21] T. Hamada *et al.*, J. Phys. Soc. Jpn. **57**, 1891 (1988).
 - [22] C. K. Majumdar and D. K. Ghosh, J. Math. Phys. **10**, 1388 (1969); **10**, 1399 (1969).
 - [23] T. Tonegawa and I. Harada, J. Phys. Soc. Jpn. **56**, 2153

(1987); K. Okamoto and K. Nomura, Phys. Lett. A **169**,
433 (1992).